Hindawi
Advances in Civil Engineering
Volume 2020, Article ID 9794756, 12 pages
https://doi.org/10.1155/2020/9794756

Research Article

A Prediction Method for the California Bearing Ratio of Soil-Rock Mixture Based on the Discrete Element Method and CT Scanning

Xiaoping Ji,[1] Jia Li,[1] Zhifei Cui,[1] Shouwei Li,[2] Yue Xiong,[3] Jianming Hu,[4] and Yingjun Jiang[1]

[1]*Key Laboratory for Special Area Highway Engineering of Ministry of Education, Chang'an University, Xi'an 710064, Shaanxi, China*
[2]*Highway Administration Bureau of Jinhua, Jinhua 321013, Zhejiang, China*
[3]*China Highway Engineering Consultants Corporation, Beijing 100081, China*
[4]*Highway Administration Bureau of Yiwu, Yiwu 321000, Zhejiang, China*

Correspondence should be addressed to Jia Li; 2018121182@chd.edu.cn

Received 13 December 2019; Revised 1 September 2020; Accepted 8 September 2020; Published 1 October 2020

Academic Editor: Chunshun Zhang

Because of the large amount of gravel with particle sizes over 40 mm in the soil-rock mixture (SRM), it is impossible to determine its California Bearing Ratio (CBR) via the indoor test method, which is a key parameter for designing the backfill in underground mined cavities or the road subgrade constructed with SRM. In this paper, X-ray computed tomography (CT) scanning and 3D reconstruction technology were used to construct the 3D structure of SRM particles with a particle size greater than 5 mm. Based on the vertical vibration test method (VVTM) and PFC^{3D}, the numerical simulation method (NSM-CBR) of SRM was established. The CBR of the SRM with a maximum particle size over 40 mm (SRM-G) was studied by NSM-CBR, and the effects of factors such as maximum particle size, soil content, and large-size particle content ($d \geq 40$ mm) on the CBR were investigated via NSM-CBR. Based on the laboratory tests and NSM-CBR, the prediction model and the determining method of CBR of SRM-G were established and verified. The results show that the maximum deviation between the CBR obtained from NSM-CBR and laboratory tests was 7.4%. The CBR of SRM-G decreases linearly with the increase in soil content and increases with the increase in maximum particle size and large-size particle content. The practical project shows that the maximum deviation between the predictive and measured values of the CBR of SRM-G was less than 1.5%, indicating that the prediction model and the method established in this paper have high reliability.

1. Introduction

The soil-rock mixture (SRM) is a heterogeneous mixture of soil particles, rock particles, water, and pores, which is widely used in highway subgrade construction in mountainous areas [1]. Due to the complexity of material composition and the irregularity of structural distribution, the SRM presents the complex mechanical properties. The California Bearing Ratio (CBR) is an important parameter of the subgrade structure design, which can well express the ability of the subgrade to resist permanent deformation; the mechanical properties of SRM are closely related to the compaction method. Moreover, the laboratory testing of SRM can only be achieved by mimicking the practical conditions. It is not economical to drill cores from a road construction site for mechanical behavior testing. Therefore, SRM samples are compacted and formed in the laboratory with the same compaction level as in the field. The correlation of mechanical properties between the laboratory-produced samples and field drilled cores is the key indicator for evaluating the quality of the laboratory compaction method. Throughout the world, forming CBR specimens is done mainly by three methods, namely, the static pressure compaction method, the shaking table method, and the surface compaction method. However, these methods of compaction do not conform to modern heavy rolling equipment, which results in low indoor standard density. The compactness can easily satisfy the requirements of the

code, which causes the unsatisfactory compactness of the soil-rock mixed subgrade and greatly affects the strength of the subgrade.

To overcome the shortcomings of the traditional methods, Chinese researchers fully simulated the effect of modern heavy rolling equipment and developed the vertical vibration test method (VVTM) based on the principle of the directional vibration roller. Compared with the traditional methods, the VVTM can reduce the optimal moisture content and increase the maximum dry density and strength of the mixtures. The correlation between the mechanical properties of an indoor test piece and an on-site core sample can reach 90%. Therefore, the VVTM has been widely used, especially in semirigid base material design [2–4]. However, the VVTM is only applicable to cohesive fine-grained soil with particle sizes below 40 mm or noncohesive free-draining giant-grained soil and coarse-grained soil. Because SRM contains a large number of particles with particle sizes greater than 40 mm (SRM-G), it is impossible to accurately determine its maximum dry density and forming specimens by the laboratory methods including the VVTM.

To solve the problem that the mechanical properties of SRM with maximum particle sizes above 40 mm (SRM-G) cannot currently be tested in laboratory tests, the virtual experiments such as the discrete element modeling (DEM) are one of the most effective solutions [5–7]. The DEM can not only complete various experimental projects as in the real environment, but also the experimental results obtained can be equivalent to or even better than those achieved in the real environment. In addition, due to its high resolution and nondestructive nature [8, 9], the numerical simulation of SRM from the microperspective based on X-ray computed tomography (CT) has gradually become the focus. Wu et al. [10] obtained the three-dimensional structure of sand via an X-ray synchrotron radiation scanner and simulated the triaxial test of sand by DEM, which verified the effectiveness of CT technology in the study of SRM. Yan et al. [11] used sphere unit and sphere unit combination to simulate soil particles and rock particles, respectively, and studied the influence of spatial distribution of soil-rock particles on SRM macromechanics. Graziani et al. [12] determined the relationship between the micro- and macromechanical properties via DEM.

It is can be summarized from the above literature reviews that the shortcomings remain in the numerical simulation of SRM. (1) The existing numerical simulation methods were mostly aimed to study the mesostructure of SRM and its impact on the macroperformance, and almost no related virtual experiments have been established for the traditional laboratory tests. (2) There are few studies on the SRM with large-size particles in engineering applications. (3) Most of the existing molding methods of SRM in DEM are still static pressure molding, and there is no research on the SRM model based on the VVTM. To addresses these gaps, the authors have performed the following work: the numerical simulation method of the VVTM for SRM (NSM-SRM) based on the DEM and CT scanning was developed; based on NSM-SRM, the CBR of SRM-G was studied comprehensively, and the CBR predictive model of SRM-G was established; the reliability of the model was verified by practical engineering.

2. Testing Methods and Materials

2.1. Test Methods

2.1.1. Vertical Vibration Test Method. To fully simulate the rolling effect of a modern heavy-duty vibratory roller, Chinese scholars [4, 13] have developed the indoor vertical vibration test method (VVTM) based on the principle of the directional vibratory roller, as shown in Figure 1. The VVTM method includes the vibration compaction method (VCM) and the vibration shaping method (VSM). The VCM was used to determine the maximum dry density and optimum water content, and the VSM was used to shape the mechanical specimens. By studying the effect of the vibration frequency, exciting force, and static pressure on the dry density of SRM, the vibration compaction parameters of SRM are recommended as shown in Table 1 [14].

2.1.2. Test of the CBR. According to the T0134-1993 bearing ratio test in "Test Methods of Soils for Highway Engineering" (JTG E40-2007) [15], the vibration forming test specimen was placed on the lifting platform of the pavement material strength tester, and the load with 45 N was applied on the penetration rod; then the dial indicator pointer of force and deformation measurement was adjusted to integer; then the initial reading was recorded. The speed of pressing in the specimen was 1 mm/min. The forces of 0.3 mm, 0.6 mm, and 1.0 mm pressure sensors on the data display instrument were recorded, and then the p-z relation curve with the unit pressure (p) as the abscissa and the penetration (z) as the ordinate was drawn. The ratio of unit pressure and standard unit pressure was obtained when the penetration is 2.5 mm as the bearing ratio of the materials, which is recorded as the CBR.

2.2. Materials.

The SRM is usually divided into soil and rock. Particles smaller than 5 mm in diameter are considered soil, and those larger than 5 mm are considered rock [16]. The soil-rock ratio is the mass ratio of soil to rock. The corresponding soil content P_5 is the mass ratio of soil to SRM by mass. The used SRM was taken from the construction site of subgrade excavation in Wuyi County, Jinhua City, Zhejiang Province. The characteristics of raw materials are shown in Tables 2 and 3.

3. Establishment of the Numerical Simulation for the CBR

The indoor CBR test method is only suitable for the mechanical property test of $SRM_{d\leq 40\,mm}$ and cannot analyze the mechanical behavior of SRM-G. Therefore, this paper presents a numerical simulation method of the CBR (NSM-CBR) for SRM-G.

3.1. Methodology to Establish the NSM-CBR for SRM-G.

The method to establish NSM-CBR for SRM-G is shown in Figure 2.

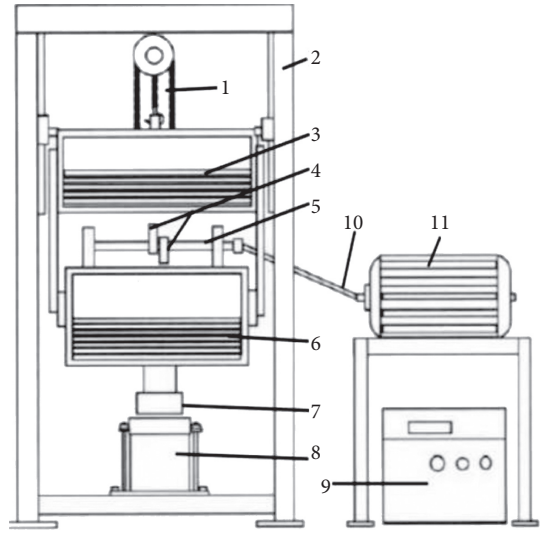

Figure 1: Vertical vibratory compactor's construction schematic: 1, lifting system; 2, frame; 3, upper system; 4, eccentric block; 5, rotation axis; 6, Nether system; 7, vibratory hammer; 8, test mold; 9, control system; 10, rotation axis; 11, electric motor.

Table 1: Vibration parameter configuration standard of the vertical vibratory compactor.

Frequency (Hz)	Amplitude (mm)	Operating weight (kg)			Exciting force (kN)	Static pressure (kPa)
		Upper system	Bottom system	Total weight		
25	1.2~1.3	107.08~115.01	170.69~179.33	277.77~294.34	5.3	154.0~163.2

Table 2: Physical parameters of soil.

Nonuniformity coefficient	Curvature coefficient	Liquid limit (%)	Plastic limit (%)	Plasticity index
13.8	1.4	30	21	9

Table 3: Mineral composition of the rock.

Mineral	Quartz	Mica	Plagioclase	Hematite
Proportion (%)	76.6	19.6	2.1	1.7

3.2. Procedures to Establish the NSM-CBR for SRM-G

3.2.1. CT Scanning of the Shape Characteristic of Rock Particles. In this paper, CT scanning technology was used to randomly collect 50 representative shape features of rock particles, obtain the digital information of the shape of the particles, and reconstruct the 3D contour of the rock particles. The experimental equipment is an industrial CT scanning device, the image reconstruction matrix is 512×512 pixels, the maximum spatial resolution is 0.02 mm, the density resolution is 0.3%, the image display matrix is 1024×1024 pixels, and the time of image reconstruction is less than 3 s, as shown in Figure 3. First, according to the coordinate matrix of aggregate surface contour points, the cloud point data of particle contour (Figure 4) were reconstructed by using the MATLAB program and converted into an STL file. Then, the STL file was used to generate the aggregate surface geometry model by using the *Geometry import* command in PFC3D, and then some spherical particles were used to fill the geometric model of aggregate to create the clump template via the command of *Clump Template* in PFC3D, so as to generate aggregate models of different shapes and sizes, as shown in Figure 5.

3.2.2. Constitutive Model of SRM. Considering the engineering properties of the materials, a linear contact model with damping was used to simulate the properties of SRM [17, 18]. The normal and tangential stiffness F_n of two contact entities in the linear contact model were realized. The contact between two entities occurred at a very small point, and only the transfer force cannot resist the bending moment, so the contact moment M_c was equal to zero. Contact force F_c was divided into elastic force F_l and inelastic force F_d. The elastic and inelastic properties of the contact elements were usually represented by the spring constant K and damper β, and the friction between particles was represented by a slider with a friction coefficient. The mechanical relationship between particle elements is shown in Figure 6.

In Figure 6, K_n and K_s represent the normal and tangential elastic constants between two particle elements, β_n and β_s represent the normal and tangential damping coefficients, respectively, and u represents the friction coefficient of the slider. The linear spring is parallel to buffer g, and

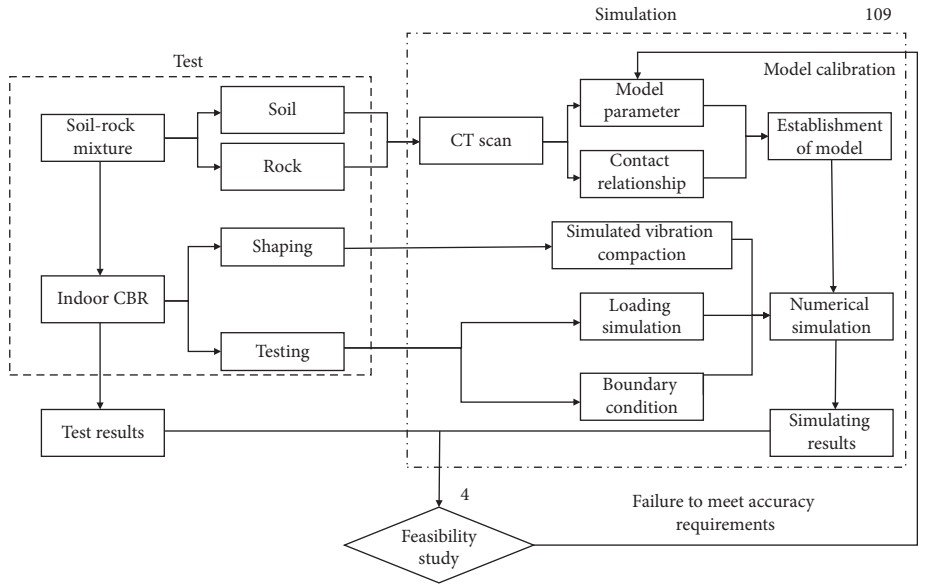

Figure 2: Methodology for establishment of the soil-rock mixture NSM-CBR.

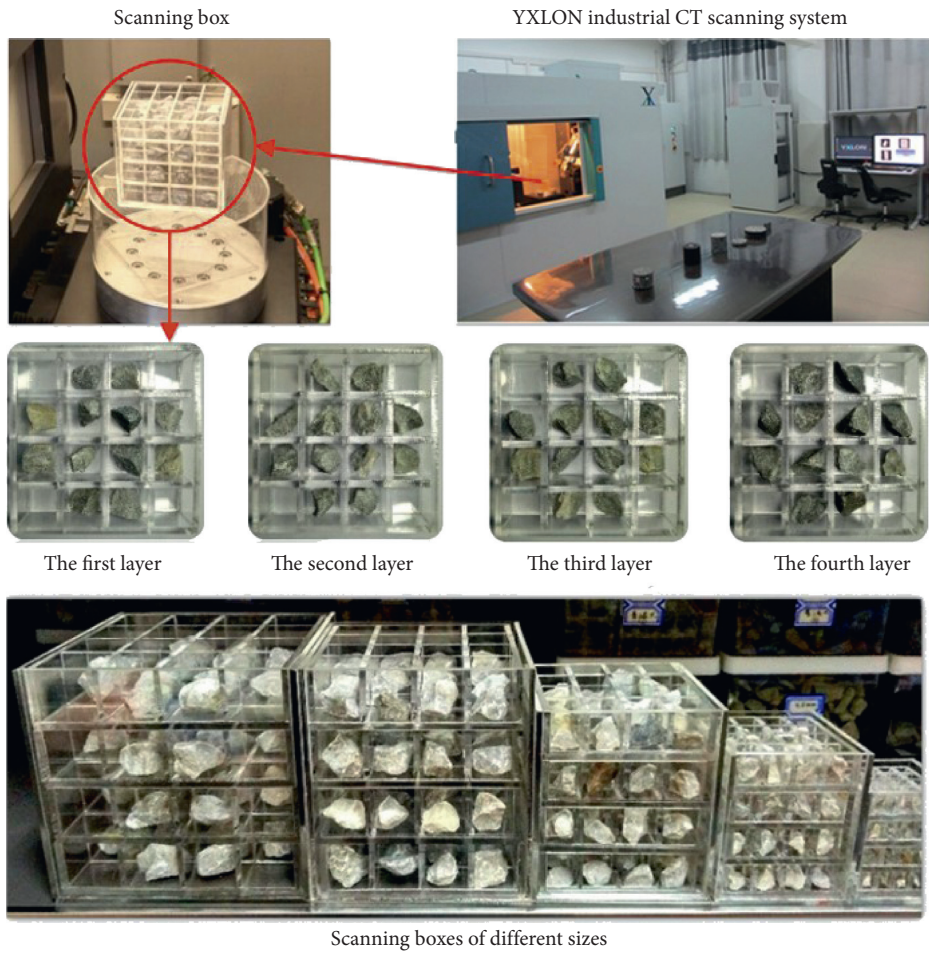

Figure 3: Scanning device schematic.

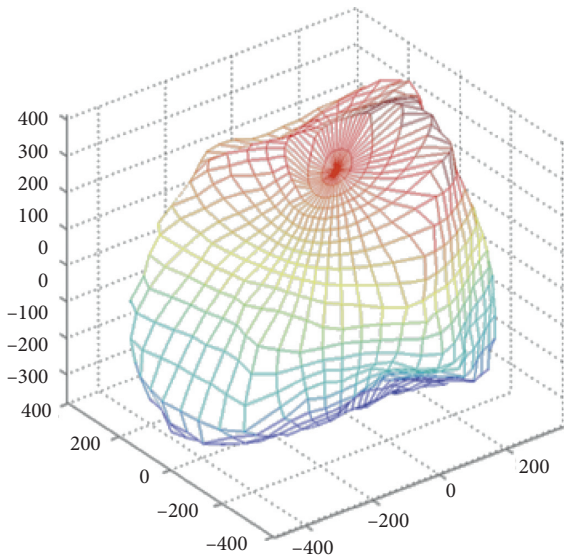

Figure 4: Particle contour.

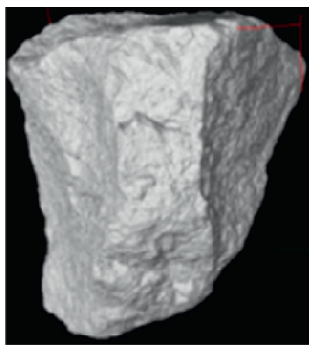

Figure 5: Three-dimensional rock particle.

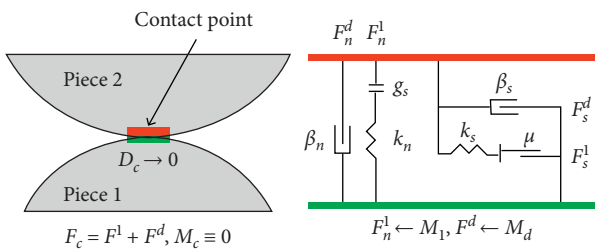

Figure 6: Physical mechanic model.

there is a gap on the surface, which is called the distance between contacts. Theoretically, the particle surface contact is shown in Figure 7. When the distance between them is less than or equal to zero, the contact surface is active.

3.2.3. Numerical Simulation for the CBR Test. According to the bearing ratio test in "Test Methods of Soils for Highway Engineering" (JTG E40-2007) [15], the CBR particle discrete element model was established.

Step 1: the model of the test tube, bearing plate, and base was generated:

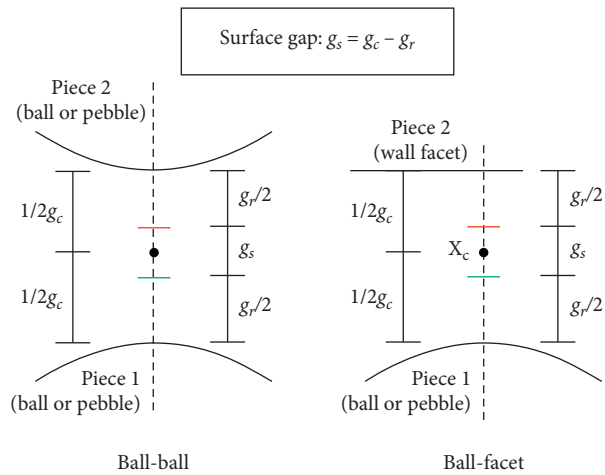

Figure 7: Schematic diagram of surface gap based on a linear model.

The modulus of the test tube, bearing plate, and base was 30 GPa, and Poisson's ratio was 0.2. The inner wall diameter of the test tube was 150 mm, the outer wall was 160 mm, and the height was 150 mm; the diameter of the bearing plate was 149 mm and the height was 25 mm; the diameter of the base was 180 mm and the height was 25 mm. The DEM model should also have the same size as the physical experiment model so that a meaningful comparison can be made between them, as shown in Figure 8.

Step 2: formation of soil-rock particles:

According to the particle composition, geometry, and physical parameters, the corresponding model was generated. The soil particle model was simplified as a sphere, and the rock particle model was input according to the CT scanning results. In order to avoid generating too many particles leading to inefficient simulation calculation, the minimum particle size of the model was controlled as 1 mm [19]. The physical parameters of the SRM are set in the PFC^{3D} simulation as shown in Table 4.

Step 3: formation of SRM specimens:

First, the gravity was applied so that all particles can reach a static equilibrium state, as shown in Figure 9. The vibration frequency was 25 Hz, the force peak was 5.3 kN, and the vibration compaction time was selected according to the compaction degree K, as shown in Table 5. Figure 10 shows the SRM virtual specimen after vibration compaction.

Step 4: determination of the CBR:

In the loading process, the load plate with a total mass of 10 kg was set first. The load of 45 N was applied on the penetration rod, and the load was started after the test piece is stable, and the force on the penetration rod was recorded. The uniaxial compression loading method was adopted in the numerical simulation. The bearing plate was loaded axially at the loading rate of

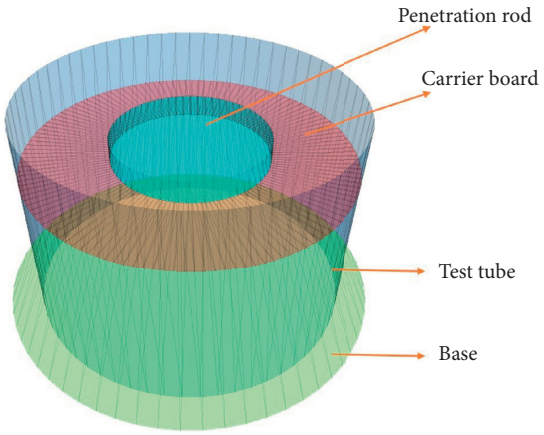

Figure 8: Discrete element model for the bearing ratio test.

Table 4: Physical parameters of the soil and rock.

Materials	Modulus (MPa)	Poisson's ratio	Friction coefficient	Damping coefficient	Bulk weight (kN/m^3)
Soil	100	0.3	0.20~0.46	0.35	2.60
Rock	20000	0.25	0.42~0.46	0.70	2.65

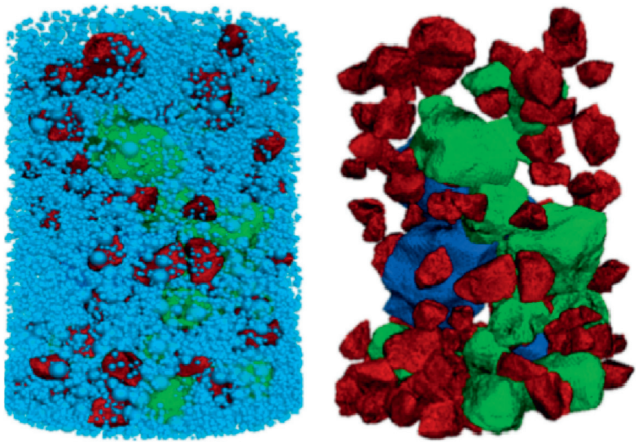

(a) (b)

Figure 9: Gravity compaction process of SRM. (a) Free fall of the mixture. (b) Arrangement of the coarse aggregate.

Table 5: Time required for vibration compaction.

Compaction degree (%)	[92, 93)	[93, 94)	[94, 95)	[95, 96)	[96, 97)	[97, 98)
Vibration time (s)	60	62	64	65	67	70

1 mm/min for 5 minutes until the penetration reached 5.0 mm; the historical records of the unit pressure (p) on the penetration rod were recorded, and the loading time was output every 30 seconds (i.e., the penetration is 0.5 mm). In addition, the penetration unit pressure p at 2.5 mm penetration was obtained, as shown in Figure 11. The CBR value of the test piece was calculated by the formula: $\mathrm{CBR} = p_{2.5}/7 \times 100\%$.

3.3. Reliability Verification. The numerical and laboratory tests on the CBR of SRM were performed for nine kinds of soil-rock ratios: 100 : 0, 80 : 20, 70 : 30, 60 : 40, 50 : 50, 40 : 60, 30 : 70, 20 : 80, and 0 : 100. The gradation of the test is shown in Table 6. The value of laboratory *CBRp* and simulation *CBRp,s* was obtained; then the cumulative relative deviation δ was calculated as the following equation:

$$\delta = \sum_{p=1}^{p} \left| \frac{CBR_p - CBR_{p,s}}{CBR_p} \right|. \quad (1)$$

During the process of numerical testing, the friction coefficient between soil particles and rock particles was

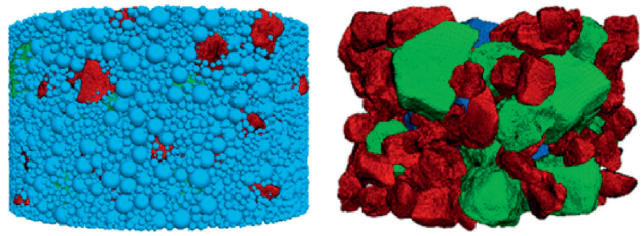

(a) (b)

Figure 10: Vibratory compaction of SRM. (a) Standard test piece. (b) Arrangement of large-size particles.

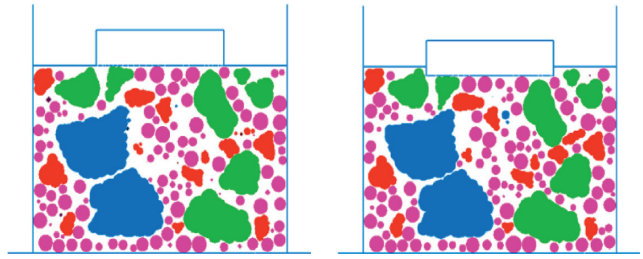

(a) (b)

Figure 11: Penetration process profile. (a) Prepenetration. (b) Penetration of 2.5 mm.

Table 6: Gradation of the SRM specimen.

Soil-rock ratio	Size (mm)				
	20–40	10–20	5–10	2–5	≤2
70 : 30	7	11	12	32	38
60 : 40	10	14	16	27	33
50 : 50	13	17	20	23	27
40 : 60	15	21	24	18	22
30 : 70	18	24	28	13	17

repeatedly adjusted. The results show that $\delta = 0.35$ reached the minimum when the friction coefficient of the rock particle is 0.41 and the damping coefficient is 0.65 and the friction coefficient of the soil particle is 0.31 and the damping coefficient is 0.34. The force-deformation curves of SRM with different soil-rock ratios obtained by NSM-CBR are shown in Figure 12, and the curve between the numerical and experimental CBR of the SRM is shown in Figure 13. The graph shows that the numerical values correspond well with the experimental values. The maximum deviation is 7.4% and the average deviation is 1.1%, which show that the NSM-CBR has high reliability. This result verifies the feasibility and accuracy of the numerical simulation and lays a foundation for the next NSM-CBR for SRM-G.

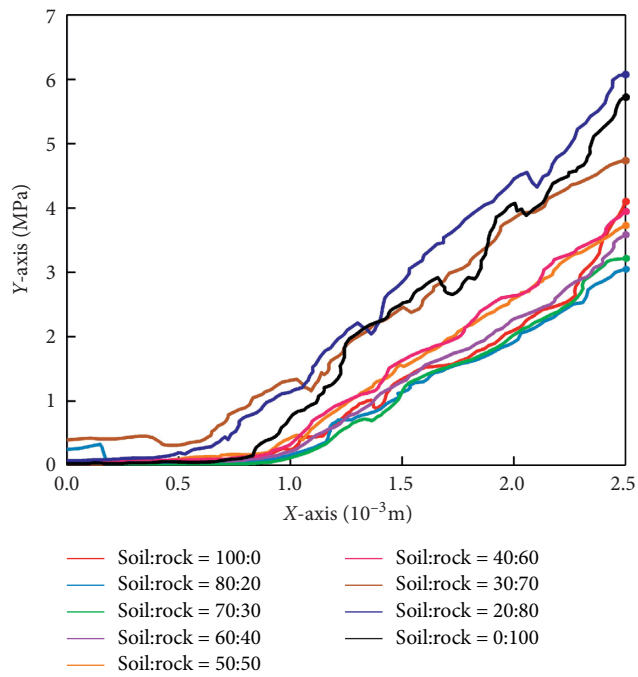

Figure 12: The force-deformation curves of SRM.

4. Application of NSM-CBR to Investigate CBR of SRM-G

4.1. Research Programme. NSM-CBR was carried out on SRM-G with three kinds of maximum particle size D_{max} (60 mm, 80 mm, and 100 mm), four kinds of large-size particle content P (0%, 10%, 20%, and 30%), and five kinds of soil-rock ratios (30 : 70, 40 : 60, 50 : 50, 60 : 40, and 70 : 30). P refers to the ratio of rock particles within 40–100 mm to SRM by mass, and the soil-rock ratio refers to the ratio of soil content to rock content by mass. The influence rules of maximum particle size, soil-rock ratio, and large-size particle content on the CBR of SRM-G were investigated.

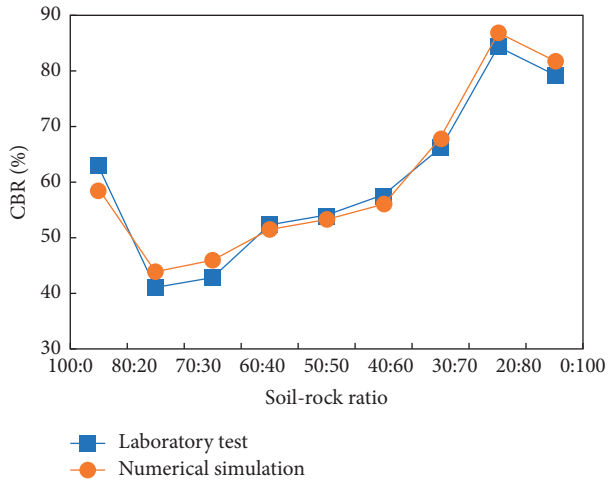

Figure 13: Contrast experiment chart.

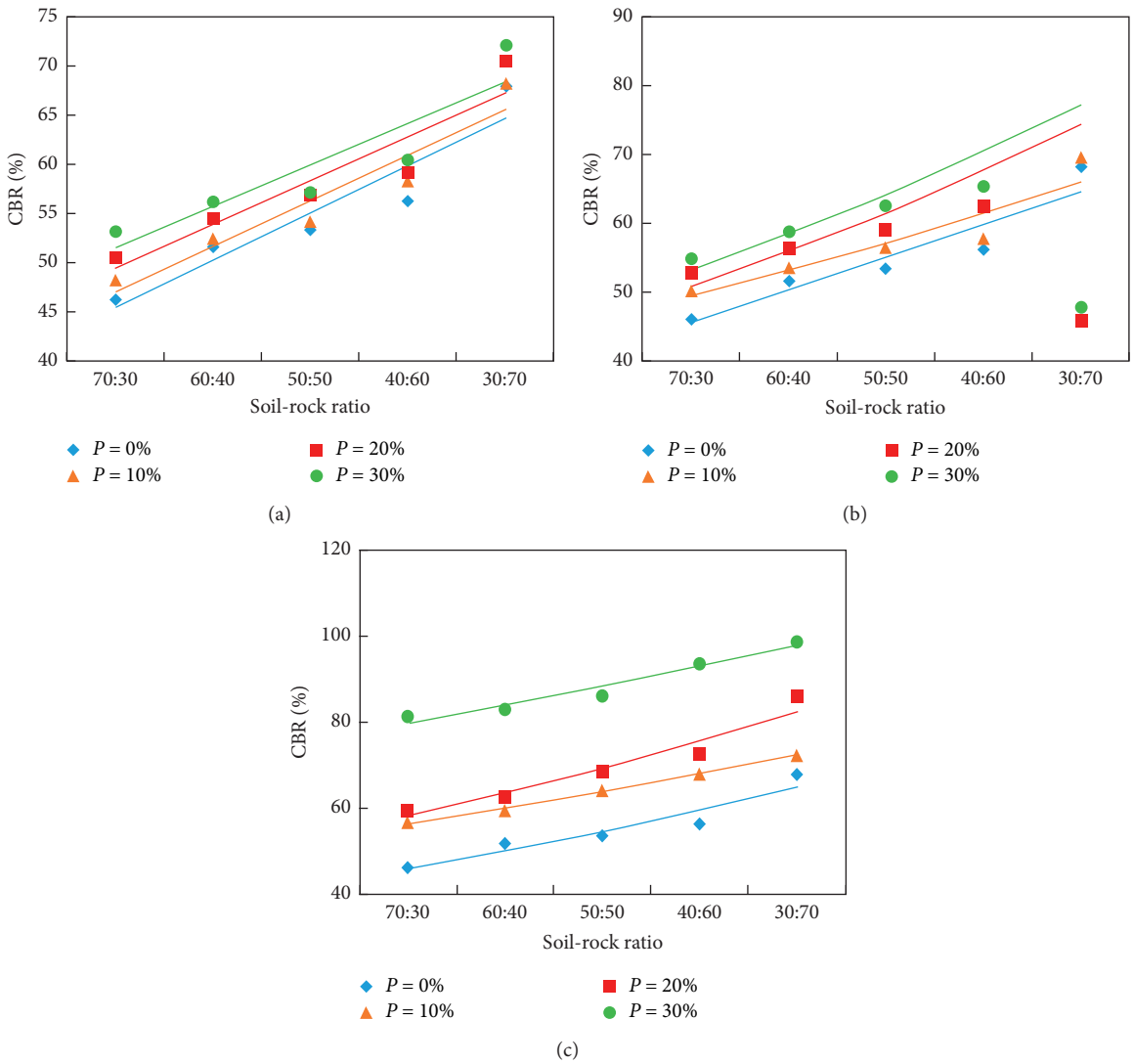

Figure 14: Variation rule of the CBR of SRM-G with the soil-rock ratio. (a) $D_{max} = 60$ mm; (b) $D_{max} = 80$ mm; (c) $D_{max} = 100$ mm.

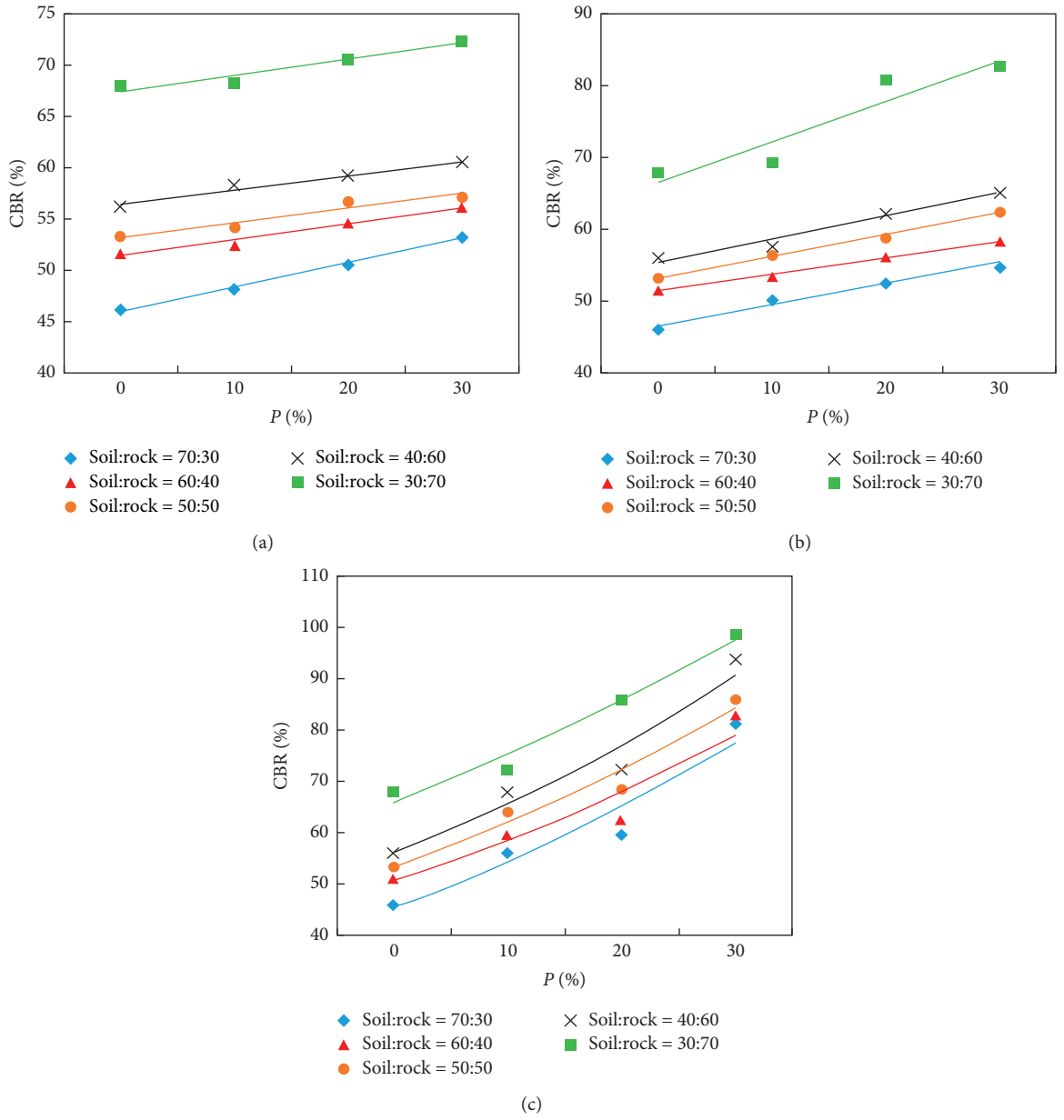

Figure 15: Variation rule of the CBR of SRM-G with P. (a) $D_{max} = 60$ mm; (b) $D_{max} = 80$ mm; (c) $D_{max} = 100$ mm.

4.2. Results and Discussion

4.2.1. Effect of the Soil-Rock Ratio on the CBR of SRM-G. Figure 14 shows the variation rule of the CBR of SRM-G obtained by NSM-CBR with the soil-rock ratio. The results show that the CBR of SRM-G increases with the decrease in the soil-rock ratio in the range of 70 : 30–30 : 70. This phenomenon can be explained from two aspects: on the one hand, with the gradual increase in rock particles, rock particles are embedded and contacted with each other to form a stable skeleton structure. The stress will be transmitted by the force chain through the contact point of rock particles, which can resist larger deformation [20]. On the other hand, the overall deformation resistance of the mixture depends on the stiffness of its constituent materials, so the CBR value of SRM-G will increase with the increase in rock particles with larger stiffness and smaller deformation.

4.2.2. Effect of the Large-Size Particle Content on the CBR of SRM-G. Figure 15 shows the variation of the CBR of SRM-G obtained by NSM-RM with large-size particle content (P). The results show that the CBR of SRM-G increases with the increase in P. The reason is that in the simulation scheme, the size of the test cylinder used is certain. In a certain range of model volume, with the increase in the content of large-size particles, the large-size particles are more likely to be close to each other to form a skeleton-like dense structure. Therefore, the contact force between particles and the CBR value can be increased.

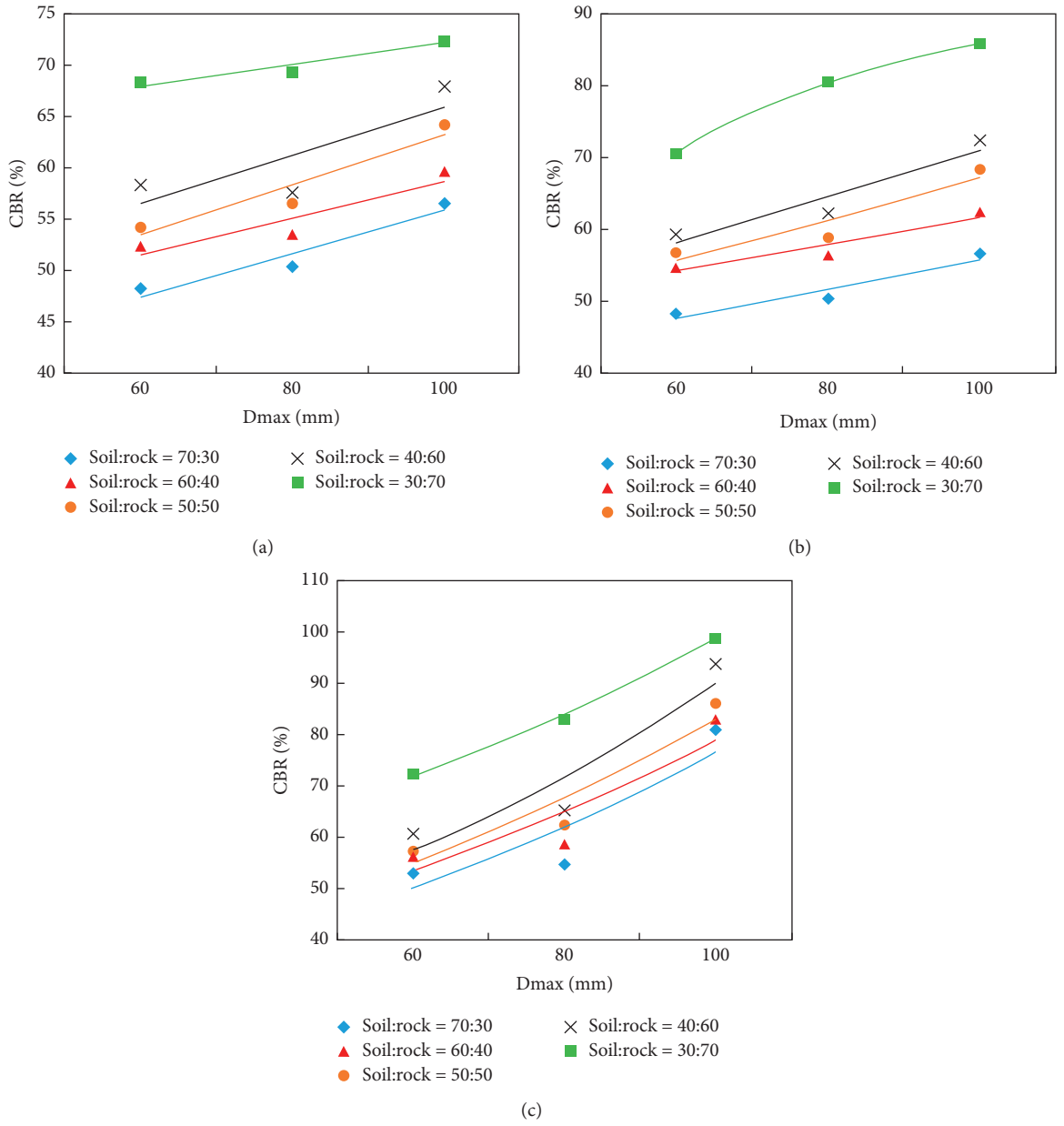

Figure 16: Variation rule of the CBR of SRM-G with D_{max}. (a) $P = 10\%$. (b) $P = 20\%$. (c) $P = 30\%$.

4.2.3. Effect of the Maximum Particle Size on the CBR of SRM-G. Figure 16 shows that the CBR value of SRM-G increases with the increase in maximum particle size D_{max}. The reason is that the SRM-G model is uniformly generated in a certain volume range, so the gradation of large-size particles is identical. With the increase in the maximum particle size, the total number of particles decreased, and the total surface area and incomplete contact among the particle decreased. As a result, the porosity decreases, the model becomes denser, and the CBR increases. It can be seen that the skeleton structure formed by large-size particles can improve the CBR value of the soil-rock mixture. Therefore, while using the soil-rock mixture to fill the subgrade, a large-size rock can be considered to enhance the permanent deformation resistance of the subgrade.

5. Prediction Model of the CBR and Its Application

5.1. Establishment of CBR Prediction Model. Given that the CBR of SRM-G has as a positive correlation and a nonlinear relationship with the maximum particle size, content of large-size particles, and CBR, a predictive model was simplified as shown in the following equation:

$$CBR = A \times CBR_{40} \times P^{B} \times D_{\max}^{C} \times P_{5}^{D}, \quad (2)$$

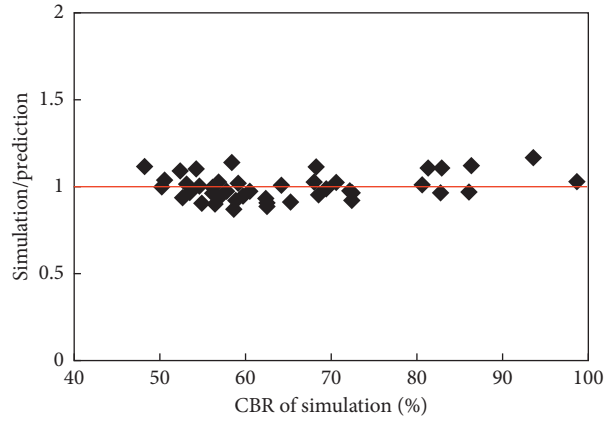

Figure 17: Comparison of the predictive and simulated CBR.

Table 7: Predicted and field testing results of the CBR.

Section	Point	CBR_{40}	P_5	P	D_{max} (mm)	Predicted CBR (%)	Field CBR (%)	Deviation (%)
	1	72.1	0.6	0.098	60	66.8	67.2	−0.4
I	2	70.4	0.5	0.125	60	67.4	68.3	1.0
	3	70.4	0.4	0.132	60	67.3	66.9	0.4
	1	66.8	0.6	0.191	80	80.1	78.6	1.5
II	2	66.3	0.5	0.204	80	79.8	80.3	−0.5
	3	68.4	0.4	0.185	80	80.1	81.6	−1.5

where A, B, C, and D are constants; CBR_{40} is the indoor-measured CBR for $SRM_{d\leq 40\,mm}$, %; P is the content of the large-size particle, %; D_{max} is the maximum particle size of SRM-G, mm; P_5 is the soil content of SRM, %; CBR is the predicted CBR of SRM-G, %.

According to the simulated results, the model parameters were calculated as follows: $A = 0.18346$, $B = 0.17317$, $C = 0.49944$, and $D = 0.04678$. The simplified prediction model of the CBR of SRM-G was obtained as follows:

$$CBR = 0.18346 \times CBR_{40} \times P^{0.17317} \times D_{\max}^{0.49944} \times P_5^{0.04678}. \quad (3)$$

To verify the validity of the prediction model for the CBR, the predictive results and NSM-RM results are compared in Figure 17. The ratio of the predicted and simulated CBR basically fluctuated around the value of 1, which showed that the prediction model has high accuracy and good predictive effect.

5.2. Determination Method of the Predictive CBR Value. The CBR of SRM-G is estimated by taking materials from the construction test section. The steps are as follows:

(i) SRM-G samples are divided into $A1$ ($d \leq 40$ mm) and $A2$ (40 mm $< d <$ 100 mm) using a 40 mm sieve; then the contents of large-size particle P and soil content $P5$ were calculated.

(ii) The maximum size (D_{max}) in $A2$ was determined.

(iii) The VVTM was carried out on part $A1$, and the maximum dry density ρ_{dmax} and optimum water content ω_{opt} of part $A1$ were determined. Then, the indoor cylindrical specimens of 150 mm × 100 mm were prepared via the VVTM according to the compactness K and determined ρ_{dmax} and ω_{opt}.

(iv) The CBR value of SRM-G was calculated by substituting the parameters CBR_{40}, P, P_5, and D_{max} into equation (3).

5.3. Field Application and Verification. The Wuyi section of Wucheng-Wuyi Highway, 235 National Road, Jinhua City, Zhejiang Province, has a total length of 4.472 km and a design standard of a two-way six-lane first-class highway. The design speed is 80 km/h. The subgrade was filled with SRM. The maximum particle size of used SRM in the test was smaller than 100 mm. The soil particles were quartzite with 42.6 MPa of the average saturated uniaxial compressive strength. There were two sections in the test. The maximum particle sizes of Section I and Section IIsec2 were 60 mm and 80 mm, respectively.

The field CBR test was carried out on two sections, respectively, according to the field CBR value test method of "Field Test Methods of Subgrade and Pavement for Highway Engineering" (JTG E60-2008) [21]. The values of the field and prediction are shown in Table 7.

The results show that the predicted value basically coincided with the field value in the field with a maximum deviation of 1.5%. Thus, the established prediction model was reliable and can provide more precise design parameters of the CBR for the design subgrade filled with SRM.

6. Conclusions

(1) The numerical simulation method of the CBR of soil-rock mixtures was established based on CT scanning and DEM. The maximum deviation in the CBR between numerical simulation and the laboratory test was 7.4%, which showed that the established NSM-CBR has high reliability.

(2) Based on the NSM-CBR, the effects of the maximum particle size, soil-rock ratio, and large-size particle content on the CBR of SRM-G were investigated. The results showed that the CBR of SRM-G linearly increased with the decrease in soil content and the increase in maximum particle size and content of the large-size particle.

(3) The prediction model of the CBR of SRM-G was established. The comparison of the predicted value and the field value showed that the maximum deviation between the two values was 1.5%. It showed that the prediction model established in this study has high reliability and can be widely applied.

Data Availability

The data used to support the findings of this study are obtained directly from the tests and included within the article.

Conflicts of Interest

The authors declare that they have no conflicts of interest.

Acknowledgments

This work was supported in part by the National Natural Science Foundation of China under project no. 51908460 and the Scientific Research of Central Colleges of China for Chang'an University under project nos. 300102219520 and 310821172008.

References

[1] W.-J Xu and H.-Y Zhang, "Research status and development trend of soil-rock mixture," *Advances in Science and Technology of Water Resources*, vol. 33, no. 01, pp. 80–88, 2013.

[2] X. P. Ji, "Study on vibration test method for soil of earth-rock mixed fill subgrade," *Highway*, vol. 64, no. 02, pp. 27–32, 2019.

[3] X. Ji, Y. Jiang, and Y. Liu, "Evaluation of the mechanical behaviors of cement-stabilized cold recycled mixtures produced by vertical vibration compaction method," *Materials and Structures*, vol. 49, no. 6, pp. 2257–2270, 2016.

[4] Y. Jiang and J. Xue, "Investigation into physical and mechanical properties of SRX-stabilised crushed rock using different compaction methods," *International Journal of Pavement Engineering*, vol. 20, no. 7, pp. 866–873, 2019.

[5] D. Bao and X. Zhang, "Granular matter and granular flow," *Journal of Zhejiang University (Science Edition)*, vol. 21, no. 05, pp. 514–517, 2003.

[6] L. Jin, "Study of effect of mesomechanical parameters on macromechanical character of soil-rock mixture," *Engineering Journal of Wuhan University*, vol. 51, no. 05, pp. 409–417, 2018.

[7] Y. X. Zhao, Z. X. Liu, and C. Mazzotti, "Numerical experiments on triaxial compression strength of soil-rock mixture," *Advances in Civil Engineering*, vol. 2019, Article ID 8763569, 15 pages, 2019.

[8] Z. Cheng and J. Wang, "Experimental investigation of inter-particle contact evolution of sheared granular materials using X-ray micro-tomography," *Soils And Foundations*, vol. 58, no. 6, pp. 1492–1510, 2018.

[9] Z. Cheng and J. Wang, "A particle-tracking method for experimental investigation of kinematics of sand particles under triaxial compression," *Powder Technology*, vol. 328, pp. 436–451, 2018.

[10] M. Wu, J. Wang, and A. Russell, "DEM modelling of mini-triaxial test based on one-to-one mapping of sand particles," *Géotechnique*, vol. 1–14, 2020.

[11] Y. Yan, J.-F Zhao, and S.-Y Ji, "Discrete element analysis of the influence of rock content and rock spatial distribution on shear strength of rock-soil mixtures," *Engineering Mechanics*, vol. 34, no. 06, pp. 146–156, 2017.

[12] A. Graziani, C. Rossini, and T. Rotonda, "Characterization and DEM modeling of shear zones at a large dam foundation," *International Journal Of Geomechanics*, vol. 12, no. 6, pp. 648–664, 2012.

[13] M. J. Li, *Study on vibration compaction characteristics of road materials*, Ph.D. thesis, Chang'an University, Xi'an, China, 2002.

[14] X.-P Ji, S.-W Li, and Y. Xiong, "Research on vibration test method for soil-rock mixture," *Highway*, vol. 64, no. 02, pp. 27–32, 2019.

[15] Transport, "Research institute of highway ministry of test methods of soil for highway engineering-JTG E40-2007," 2007.

[16] Y. Dong, "Experimental study on intensity character of rock-soil aggregate mixture," *Rock and Soil Mechanics*, vol. 06, pp. 1269–1274, 2007.

[17] Y. L. Tu, *The macro and meso mechanical characteristics and nonlinear elastoplastic constitutive model of soil-rock aggregate*, Ph.D. thesis, Chongqing University, Chongqing, China, 2017.

[18] P. Wang, "Soil-rock-mixture large-scale triaxial test and mesoscopicmechanics characteristics of pfc simulation,"-Master thesis, Chongqing University, Chongqing, China, 2017.

[19] Yu Li, L. Li, and K. Chen, "Study on the relationship between particle size distribution and stress-strain of soil," *Journal of Railway Science and Engineering*, vol. 15, no. 07, pp. 1722–1729, 2018.

[20] L. Fan, "Study on the rapid detection method of compaction quality with earth-rock subgrade based on PFWD,"Master thesis, Chang'an University, Xi'an, China, 2011.

[21] Transport, "Research institute of highway ministry of, filed test method of subgrade and pavement for high engineering-JTG E60-2008," 2008.